PROCEEDINGS, 50th Workshop on Geothermal Reservoir Engineering
Stanford University, Stanford, California, February 10-12, 2025
SGP-TR-229

Numerical Modeling of Casing-Cement Failure in Geothermal Wells Using Modified CZM Bonding Conditions

Ionut LAMBRESCU[1], Elvin ALLAHVERDIYEV[2], Khizar ABID[2], Catalin TEODORIU[2]

[1]Petroleum-Gas University of Ploiesti, Ploiesti, Romania

[2]Mewbourne School of Petroleum and Geological Engineering, The University of Oklahoma, Norman, OK, USA

cteodoriu@ou.edu

Keywords: FEM, casing-cement, CZM, geothermal well failure mechanism.

ABSTRACT

Experimental testing of casing-cement debonding has shown that a remaining axial force similar to friction is noticed after shear debonding. This cannot be explained using pure CZM models since no normal force exists after debonding; thus, the friction force should have been zero. A modified boundary condition scenario has been created to understand this phenomenon better. A CZM model is used until the debonding is created, after which the stress conditions are transferred to a friction bonding model between cement and pipe. The results have shown that the remaining friction force can be significant and may justify limited wellhead growth in geothermal wells due to thermal expansion. The paper will show the numerical model and the simulation results modeled around a synthetic geothermal well. The results will help well design engineers improve short- and long-term well integrity and better wellhead movement prediction.

1. GEOTHERMAL WELLHEADS

Given its prospective for sustainability and continuous supply, geothermal energy presents special engineering challenges, especially when it comes to wellhead system design and maintenance. Except offshore HPHT (high-pressure high-temperature) wells, these difficulties are generally rare in the oil and gas sector. The temperature of the fluids produced in geothermal wells differs drastically from that in oil or gas wells (Godare, 1978). A geothermal wellhead is a specialized wellhead used for steam wells. While the basic structure is similar to oil and gas wellheads, geothermal wellheads may adhere to additional standards. Typically, oil and gas wellheads are designed and manufactured according to API Spec. 6A standards. However, for geothermal wellheads, the master valve is typically produced according to API Spec. 6D standards.

In geothermal well engineering, the term wellhead is used in two different contexts. The first context is the drilling wellhead, which is set up after the surface casing and is succeeded by each subsequent casing head. The second context is the final or permanent wellhead, which is generally placed on top of the anchor casing, although in some situations, the production casing acts as the anchor casing (Unit, 2016). The expansion spool is unique to geothermal wellheads and is commonly used in wet steam applications. It accommodates the inevitable expansion that occurs during thermal cycling. The wellhead can stay stationary thanks to the expansion spool, which also lessens the strain on the steam-gathering system (Williams, 1991). Using the expansion spool is a long-standing practice in the Philippines, New Zealand, Iceland, and the United States. According to Gunnar Skulason Kaldal et al. (2015), the majority of Icelandic geothermal wells have the production casing sliding inside an expansion spool beneath the wellhead's master valve, while the wellhead is attached to the anchor casing. The expansion spool accommodates the thermal expansion of the casings and wellhead assembly (Atlason et al., 2015). It allows the production casing to expand freely without causing the wellhead to move (Þórhallsson, 2003).

Gunnar Skúlason Kaldal et al. (2015) state that the anchor casing is connected to the expansion spool below the master valve to allow axial displacement of the production casing inside the wellhead when it expands thermally. The concrete and casing strings experience thermal stress due to thermal expansion. Under full casing constraint, the thermal stress is approximately 10.7 psi/°F (or 2.5 MPa/°C). When the temperature rises during the well's first production, thermal strains may build up to the casing's yield strength, causing plastic strain to occur. Since plastic strain is permanent, tensile forces will develop in the casing if the well cools down again. The casing may fail as a result of these tensile stresses if they exceed the coupling joint strength of the casing.

The dominant dissolved gases in geothermal wells are typically CO_2 and H_2S. During production, wellhead equipment can wear out or begin to corrode. Key valves may experience internal defects and a decrease in wall thickness over time, which could result in well control failures. Especially the presence of H_2S in produced fluids may necessitate sour service metallurgical specifications. Elevated geothermal temperatures can also lead to a 17% reduction in wellhead equipment pressure ratings at 300°C (572°F) under the ANSI Standards (Hole, 2008). Figure 1 shows the wellhead working pressure de-rating for flanges and valves according to ASME (2010) and Institute (2011).

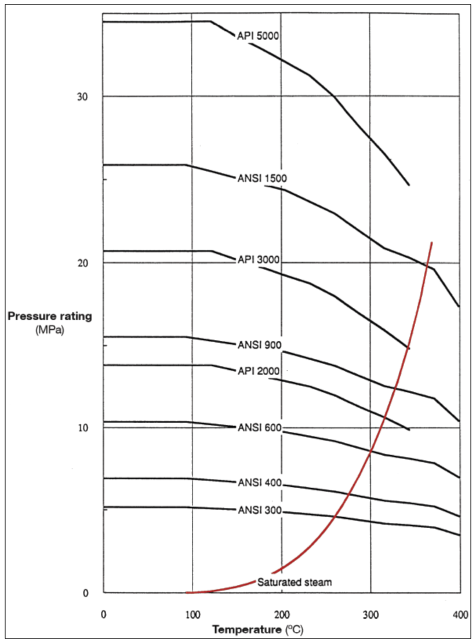

Figure 1: Wellhead working pressure de-rating for flanges and valves according to ANSI B16.5 and API 6A (Unit, 2016).

Surface and conductor casing strings are used to support the initial drilling wellhead. According to Hole (2008), the final permanent wellhead is attached to the anchor casing. The casing head flange (CHF) is typically attached to the top of the anchor casing, but in some instances is directly connected to the top of the production casing (Hole, 2008). A CHF is a flange installed to the anchor casing, serving as the attachment point for the permanent wellhead. If the wellhead is secured to the production casing, then this casing is known as the anchor casing. The surface casing is the initial casing that supports the drilling wellhead. The ultimate wellhead may be mounted on the innermost production casing/tieback or a shallower intermediate casing. In each scenario, the casing that the final wellhead is attached to is defined as the anchor casing. The components of what is termed the permanent or final wellhead consist of the outer flanges of the master valve that are directly exposed to the fluid at the top of the well, the outer flanges of the primary side valves that are also directly exposed to the fluid, and the bottom of the casing head flange that connects the wellhead to the casing, along with any spools or additional components found between these elements (Unit, 2016). According to Kruszewski et al. (2017), the CHF can also be mounted to the top of the production casing, eliminating the need for an expansion spool.

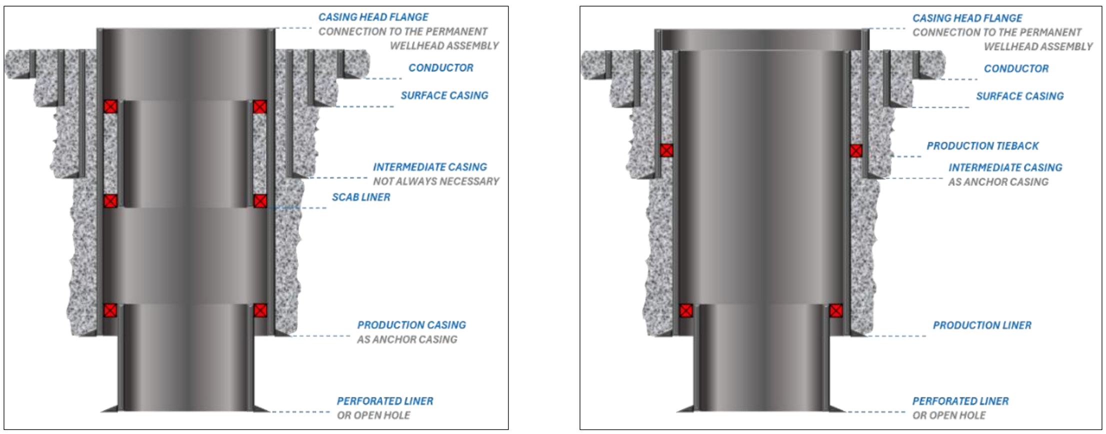

Figure 2: Typical geothermal well completion schematics. (Left) well completion with production casing completed as anchor casing (Unit, 2016). (Right) well completion with intermediate casing completed as anchor casing (Hole, 2008).

The CHF may possibly incorporate side outlets to which the side valves are attached. The final wellhead also includes a double-flanged expansion/adaptor spool. Side outlets may be connected to the expansion spool as an alternative to those on the CHF. Most importantly, the final wellhead includes a master valve (Hole, 2008). Figure 2 provides two schematics of typical well configurations for geothermal wells according to Unit (2016) and Hole (2008). An intermediate casing can additionally be run between the production and anchor casing. The necessity of this intermediate casing depends on the vertical temperature profile (Watson, 2013).

In New Zealand, geothermal wellheads are placed in concrete cellars to contain the spills of drilling fluid and facilitate wellhead maintenance. Casings terminate at the cellar floor, with extra length cut off during construction. The anchor casing remains above the cellar floor, supporting the CHF, to which the master valve and wellhead assembly are mounted. Pressure within the well generates upward forces that may lift the anchor casing when the valves are closed, known as lift-off. After completion, the CHF becomes the reference point for depth measurements. Over time, the CHF may rise due to thermal expansion, typically ranging from 0.39 to 3.9 inches (or 10 to 100 mm) (Watson, 2013).

2. WELLHEAD GROWTH

According to Hole (2008), despite cementing efforts, there is usually residual axial thermal expansion between casing strings at the surface. If the wellhead is attached to the anchor casing, movements of the production casing relative to the anchor casing are accommodated below the master valve in a double-flanged expansion spool to avoid interference. The fluid at the geothermal wellhead may be superheated steam, saturated steam, water, cold gas, or mixtures. Surface conditions typically differ from downhole values but may approach them in some cases (Hole, 2008). According to Unit (2016), the geothermal wellhead design must allow the uppermost 82 feet (or 25 meters) of each casing string to expand within its temperature range without obstruction.

Strict tolerances are applied to the "well foundation" in the oil and gas industry, including the conductor and surface casings, to accommodate any cement shortfall behind the surface casing. Foundation design varies with well construction operations and intended use (i.e., production or injection) due to differing thermal load effects. Surface casing in onshore wells is typically cemented to the surface (Cutrim et al., 2021). To reduce well construction costs, surface casing shoes may be set deeper, complicating the primary cement job, especially in formations prone to lost circulation. Ironically, most geothermal wells are drilled to normal or subnormal pore pressure formations.

The extent of wellhead movement (WHM) is significantly dependent on the intensity and duration of thermal loads. Temperature changes in the wellbore can cause the casing strings to expand or contract significantly, leading to a large vertical WHM. The thermal stress primarily arises from uncontrolled heat transfer from the tubing to the casing strings (McCabe, 1989). Since most of the geothermal wells are completed tubingless, hot production could directly undergo the casing strings to thermal loading. Apart from thermal loads, the wellhead position can also be gradually shifted by geological factors (McCabe, 1989).

Thermal movement can be caused by both short- and long-term loads. This includes the shrinkage of water and geothermal injectors, and the expansion of geothermal producers. The thermal expansion is particularly critical in cold regions where hot water is injected or produced (Gao et al., 2016; Liang, 2012). Typical allowances for the WHM are 10 inches for oil producers and 20 inches for gas injectors (McCabe, 1989). According to Sathuvalli and Suryanarayana (2016), flowline design must also consider the associated stresses when the WHM ranges from 6 to 12 inches.

In onshore wells, the conductor is generally cemented to the surface and not connected with the wellhead, but load sharing can occur between the conductor and surface casing via the base plate. Environmental and industry standards mandate cementing the surface casing to the surface to isolate the freshwater aquifers and directly support wellhead loads. Production casing string may be top-cemented, while liner strings do not participate in wellhead growth (Gao et al., 2016).

In typical geothermal wells, only the anchor casing is connected to the wellhead, and the well is usually cemented to the surface. When injecting or producing steam or hot water, the wellbore heats up, causing the cement sheath to separate from the casing, which leads to wellhead growth. When hot injection or production stops, the casing shrinks, and the wellhead returns to its original position, potentially even subsiding (Gao et al., 2016). The wellhead growth is more severe in high-temperature wells in cold environments, where temperature changes are more significant (i.e., between the operating and the as-installed condition) (Liang, 2012). In onshore wells, where the conductor is cemented to the wellhead, thermal force on the wellhead may reach its maximum with zero wellhead growth since the conductor has a large cross-sectional area (CSA), making it stiffer than the combined stiffness of all inner strings (Liang, 2012).

Wellhead growth is primarily caused by thermal stress on the casing strings connected to the wellhead (Liang, 2012). The wellhead acts as a rigid body, with the surface, intermediate, and production casings expanding simultaneously due to thermal expansion. The stiffness of the surface casing is much greater than that of the others, so significant wellhead growth indicates that the surface casing must have a significant section moving axially. A high-quality cement job freezes the axial tension in the casing, fixing it and preventing its axial movement. This tension depends on the size of the casing, density of the slurry, displacement fluid, and holding pressure cement cures. Sufficient bonds between the casing(s) and cement sheath are required to withstand thermal stress. If the surface casing has a free section before production, or if the cement sheath fails due to poor quality of the cement job, the top axial force will be zero, and the free section must self-stand. Axial force changes with subsequent loads on the wellhead, and a poor cement sheath cannot support axial loads, causing separation from the casing (Gao et al., 2016; Liang, 2012). The stress from expanding strings can crack existing bonds between the cement and casing (Almulhem et al., 2020). Without a free section of surface casing before production, wellhead growth is unlikely during production (Gao et al., 2016). Assuming the cement sheath fails before production, the wellhead grows upwards with increased wellbore temperature during production. Thermal growth may shear the wellhead locking pins, so their total shearing capacity must meet the thermal operational load conditions (Liang, 2012). A top-quality cement job is crucial, and an enhanced base plate should bear the wellhead load, placed on the ground rather than on the conductor. If wellhead growth is detected during production, a bracket should support the wellhead, be placed on the ground, and strictly control flow rates (Gao et al., 2016).

Casing strings are installed in the well with an as-installed landing load at the wellhead. Slack-off or pick-up loads during installation will reside in the wellhead landing shoulder: slack-off reduces compression, while pick-up increases it. During production or injection, additional loads (compression or tension) are added to the wellhead. If there is an as-installed compression load, thermal force must overcome this before exerting an upward force on the wellhead. The weight of the wellhead and production tree, which adds downward compression, must also be considered. Poor cement job quality, cement channeling, annular fluid expansion, and omission of pick-up forces during installation can all contribute to wellhead growth (Gao et al., 2016).

During hot production phases, cement bonding prevents the thermal expansion of casing strings but places significant stress on the cement to resist vertical movement. Shutting in the well causes temperature decreases and thermal shrinkage of both cement and casings, returning the well to its as-installed state. According to Almulhem et al. (2020), several production and shut-in cycles can deteriorate the cement bonds, which may eventually worsen the issues developing due to thermal expansion. Microchannels may be generated in the cemented annuli due to this, which may also lead to high sustained annular pressures if there is a connection to the contaminated pockets or permeable zones. Fluids typically infiltrate these microchannels during cooldown periods after production in HPHT and geothermal wells. Although the formation pressures are lower in geothermal wells, trapped fluid expansion within the cement channels during subsequent heating cycles can result in challenges during subsequent production periods (Almulhem et al., 2020).

Control over the thermal expansion of casing strings is necessary if not the most important due to the potential challenges it may lead to in terms of wellhead and surface infrastructure integrity, pipeline damage, structural beam collisions, and wellhead access blockage. One of the most critical concerns is the connection between the Christmas tree manifold and the flowline flange (Almulhem et al., 2020). The Christmas tree may be tilted due to wellhead growth, which is because there is an anchoring effect between the fixed flowline and the tree. If this happens, there may be safety hazards, surface flowline damage (i.e., line ruptures), and the risks of well integrity issues (Proano et al., 2023). The wellhead and the stiff flowline, which is attached to the tree, might not move at the same rate (Almulhem et al., 2020). Flexible components might be added to the flowline to lessen these problems. These problems can be successfully avoided with thermal wellheads, which can allow for an expansion of roughly 19 inches through the casing spool (Proano et al., 2023).

It is believed that there will be some looseness between the top of the string and the soil, even in fully cemented threads (Sathuvalli & Suryanarayana, 2016). The height of this looseness below the mudline or ground level is called the POF (point of fixity). Thus, below the POF, the casing string has zero displacement and is in full contact with the formation or cement. Depending on the shear stress profile at the interface of the structural casing and soil, the POF of the structural casing might be below the mud line, leading to motion in the subterranean section. When a hot shut-in well cools, thermal forces vanish, but the wellhead may not return to its original position due to anisotropic frictional forces, leading to ratcheting (gradual upward movement). This is critical when the net thermal force on the wellhead approaches or exceeds the pullout capacity of the structural casing (Sathuvalli & Suryanarayana, 2016).

If soil quality is inadequate, the conductor may be drilled and cemented. The surface casing can also serve as the structural casing. Depending on where the wellhead high-pressure housing is mounted, the upward forces created by the inner tubular during production can pull the structural casing out of the ground. This force must be resisted by shear stresses between the lateral surface of the structural casing and the formation or the cement sheath. The final WHM is determined by the net upward force, structural casing stiffness, and subsoil resistance (Sathuvalli & Suryanarayana, 2016).

In fully cemented offshore wells, wellhead growth can still occur, risking leakage, accelerating casing corrosion, and damaging wellhead equipment. Annulus pressure from temperature effects and other forces acts at the top of the annulus. This pressure affects both the casing head, causing casing growth, and creates a radial gradient pressure on the inside and outside walls of the casing due to the liquid column pressure. After cementing, a dense cement sheath forms between the casing strings and the formation. The bonding strength at these interfaces is crucial in resisting wellhead growth and depends on thermal stresses, annulus pressure, and formation stresses (Zhang et al., 2017).

Wellhead growth is influenced by the damage between the formation-cement or cement-casing interfaces, if applicable. If there is damage between the cementing interfaces, the wellhead may grow, or it will resist the growth. Growth may occur if the lifting force exceeds the cementation force. Any damage to the interfaces of cement can reduce the cementation force and eventually the frictional resistance. That is why it may become easier for the wellhead to overcome the reduced frictional resistance, which correlates with vertical stress, and grow upwards (Zhang et al., 2017).

Zhou et al. (2024) suggest an approach for assessing the bonding performance at the casing-cement sheath contact interface, which helps determine the strength of the radial and axial bonding, as well as the friction coefficient at the cementing interfaces. The findings indicate that the failure of cement sheath integrity is the main reason why WHM may happen in fully cemented wells (i.e., cement slurry returns to the wellhead). Zhou et al. (2024), in their study, mention three different types of cement sheath failures: deterioration of the cement strength due to high temperature; failure within the cement and interface debonding because of the cyclic thermal loads; and the dissolution of cement that is exposed to corrosive fluids (e.g., CO_2 and H_2S).

2. METHODOLOGY

The calculation theory in the first part of the results uses a multi-string tubular design software based on the works of Halal et al. (1997) and McSpadden and Glover (2009). The WHM analysis begins with the undisturbed conditions for the outermost casing string and applies all loads sequentially up to the final load. Because the loads are dependent, it is important to consider all loads accurately. The outermost casing is the string to which the wellhead will be attached. All inner strings, including the outermost casing, are part of the total system stiffness and subsequent axial load events. String stiffness is influenced by factors such as CSA, Young's modulus, and string length (Equation 1).

$$k_i = \frac{EA_i}{L_i} \tag{1}$$

Where

k_i = stiffness (lbf/in)

E= Young's modulus (psi)

A_i = string cross-sectional area (in^2)

L_i = uncemented string free length (in)

Initially, the approach to analyze the WHM focuses on the TOC behind the casing strings. The data to conduct this study was obtained from a reference well belonging to the FORGE project (McLennan, 2022; McLennan et al., 2021; Winkler et al., 2021). Table 1 presents the casing configuration of the corresponding well.

Table 1: Casing and hole configuration of the simulated well.

Well Configuration	OD, in	Weight, ppf	Grade	Connection	TOC, ft	Shoe, ft	Hole Size, in
Conductor	20	54.0	B	Welded	Surface	130	26
Surface	13-3/8	68.0	L-80	BTC	Surface	1629	17-1/2
Intermediate	9-5/8	40.0	HCL-80	BTC	Surface	5132	12-1/4
Production	7	38.0	T-95	JFELION	Surface	10787	8-3/4
Open Hole						10987	8-3/4

Both cold pump-in and hot flowback have been simulated (Figure 3), whereas the study will focus on wellhead growth due to hot production. While WHM may also result from other operations, such as nipple-up BOP, the primary focus is on understanding the thermal-induced loads on the wellhead. The period for hot production was set at 10 years. Although assuming that the maximum wellhead temperature will approach the undisturbed bottom hole temperature might be conservative, this scenario is unlikely without thermal insulation, such as vacuum-insulated tubing (VIT). Thus, this should be regarded as a calculated risk. Figure 3 presents the life-of-well temperature profile for the casing strings under cold injection and hot production.

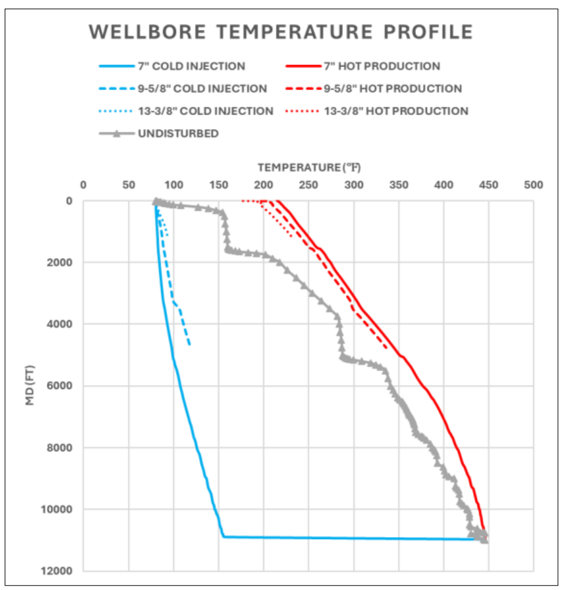

Figure 3: Wellbore temperature profile for the simulated well. Separate casing temperature profiles for cold injection and hot production.

If it is assumed that all casing strings are uncemented, then the string stiffness would reduce in this sequence according to Equation 1 and Table 1: conductor, surface casing, intermediate casing, and production casing. Thermal-induced WHM would occur due to the uncemented part of a casing string connected to the wellhead and weak cement bonds (i.e., good cement was assumed in the first part of the results). Thus, if the uncemented length of the string increases, its stiffness value will automatically be reduced. The same can be said about the strength of the cement bond. This study does not include lift-off assessments or the potential unseating of any casing string from its previous position.

In the analysis of WHM, it is also crucial to specify the outermost casing string to which the wellhead will be attached. In this sensitivity study, the wellhead was attached to the surface casing string. It is also important to note that all drilling events occurring before the setting and cementing of the designated outermost casing string do not affect the WHM analysis. The primary goal of this study was not to evaluate drilling loads, which include static, landing, and thermal loads, but rather to understand the thermal loads induced by production activities. The total length change of surface and production casing strings have also been hand-calculated to compare with the simulation results. An uncemented length factor "Q" is introduced to the thermal length change calculation (Equation 2).

$$\Delta L_{temp} = \alpha Q \Delta T_{avg} L \tag{2}$$

Where

ΔL_{temp} = length change due to temperature (in)

α = coefficient of thermal expansion (°F^{-1}) = $6.9\text{x}10^{-6}$ °F^{-1} for steel

Q = uncemented length factor (%)

ΔT_{avg} = average temperature change (°F)

L = string length (in)

3. RESULTS

3.1. WELLHEAD GROWTH VS. TOC REDUCTION

Figure 4 presents the wellhead growth as a function of TOC reduction for two operations, namely, hot production and hot shut-in. The hot shut-in duration was assumed to be 6 hours after the stop of production. The wellhead was simulated to be attached to the surface casing, which was designated as the outermost string. The amount of wellhead growth was determined based on the TOC level behind the surface casing, and all inner casing strings had cement to the surface.

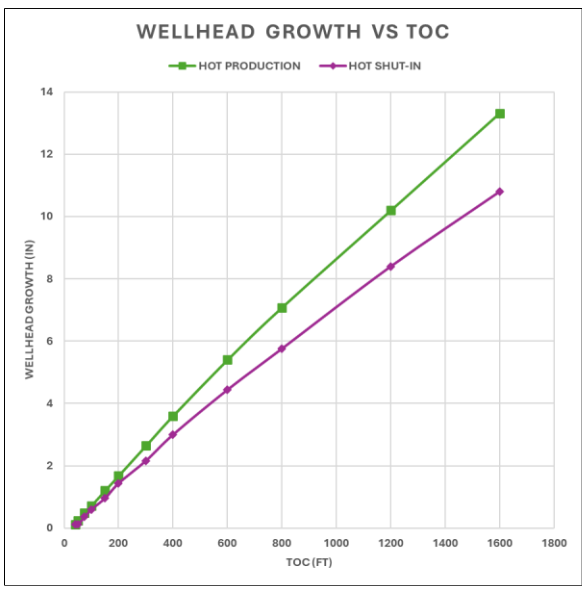

Figure 4: Wellhead growth under 10-year hot production and post-production hot shut-in for 6 hours. The amount of wellhead growth was determined based on the TOC level behind the surface casing.

During hot production operation, the casing will expand when it is heated, which leads to compressive axial stresses. The wellhead grows up linearly with the reduction in TOC. The plot indicates that the wellhead growth would be higher when the TOC is reduced further. Overall, the thermal expansion effects are more noticeable during hot production compared to shut-in. The hot shut-in leads to slightly less growth because of the reduction in producing temperatures after 6 hours. This trend shows that the wellhead growth due to thermal expansion remains significant even during the 6-hour shut-in period. Once the well is shut in, temperatures within the wellbore begin to decrease. The extent of this temperature reduction is dependent on the duration of shut-in, and it may even take weeks or months to return to the original geothermal temperature profile after the 10-year hot production operation. A linear dependency is seen between the steel thermal expansion and the free length of the casing string. Figure 5 compares the simulated and calculated wellhead growth in terms of the 13-3/8" surface casing uncemented length factor "Q". The total length change was calculated using Equation 2. Slight differences can be observed in the calculations that assume average temperatures rather than a complete temperature profile.

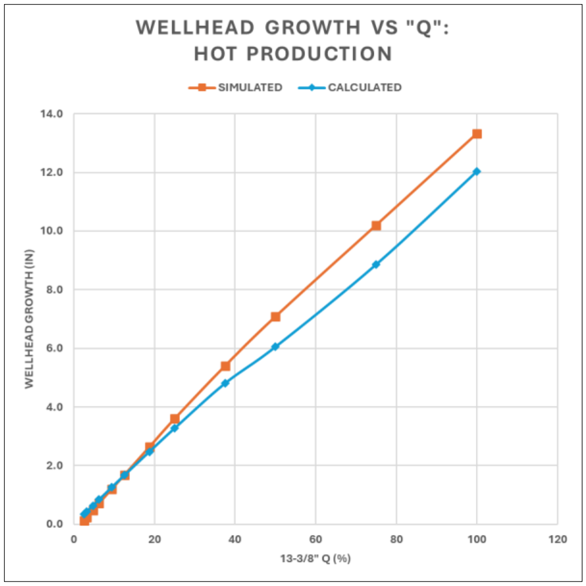

Figure 5: Wellhead growth under 10-year hot production due to the total length change of 13-3/8" surface casing. The amount of wellhead growth was determined based on the uncemented length factor "Q".

3.2. MODIFIED CZM BONDING

Modeling the casing-cement bonding with CZM implies the use of bilinear law (Figure 6), where T_n^{max} is the maximum tangential cohesive traction τ_{max} and δ_t^c is the tangential displacement jump at the completion of debonding. These values are determined experimentally. This approach is expected to produce a behavior when δ_t^c is reached, the casing will be free to move since the initial bonded with CZM contact between casing and cement changes to frictionless or frictional contact. Since there are no normal loadings, able to produce friction, in this case, the contact will be frictionless. To summarize, after contact debonding, a jump in the casing displacement will appear.

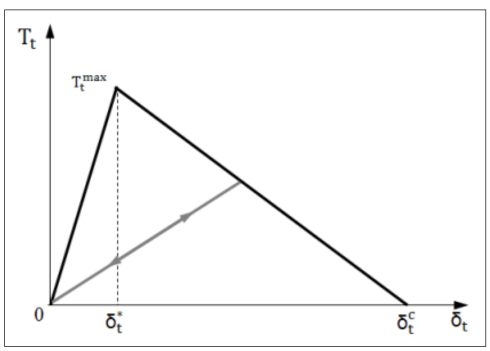

Figure 6: CZM bilinear zone.

Such a situation is presented in Figure 7, where the casing is subject to a load of 48,000 N. The CZM properties have been derived from the lab test (Figure 8):

- Maximum Equivalent Tangential Contact Stress – 2.085 MPa;
- Tangential Slip at the Completion of Debonding – 7.5 mm

A Mode II (shear) debonding has been considered, with no temperature.

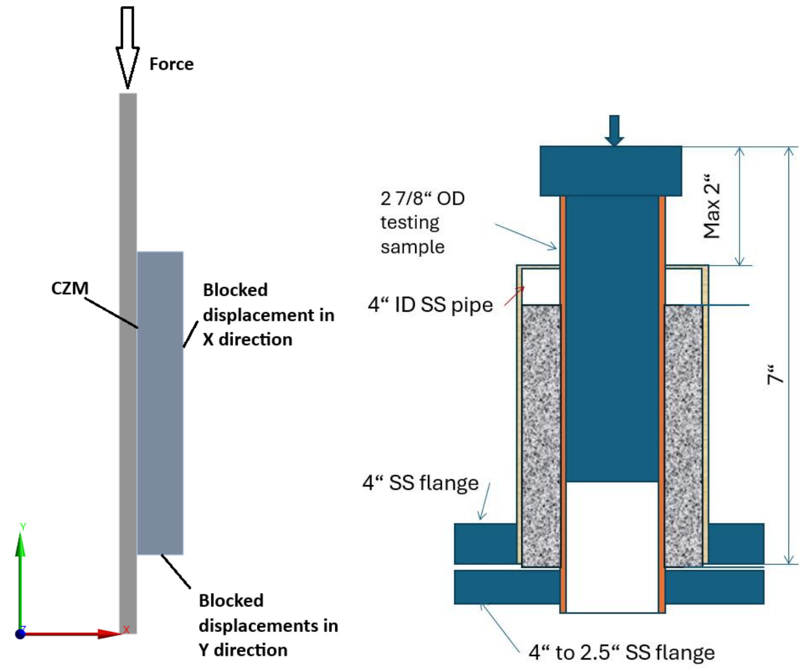

Figure 7: Model for the FEM analysis and setup.

In order to capture the debonding process, two results are the most conclusive: the axial displacement (of the casing) and the reaction force at the cement base (where the Y displacement has been blocked – see Figure 7 left).

In Figure 9 the reaction force variation is captured.

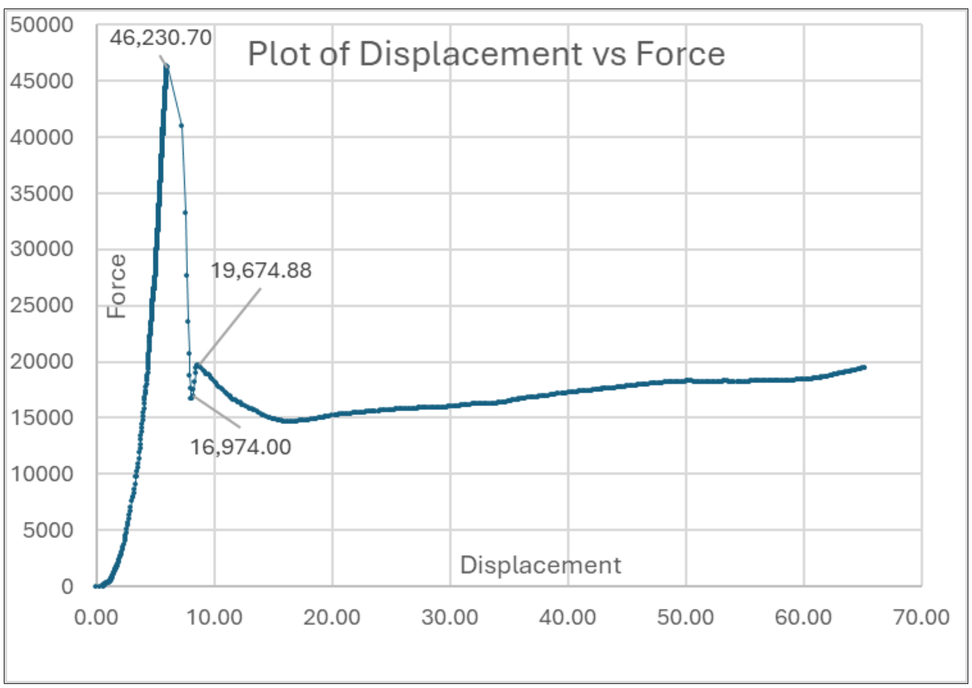

Figure 8: Plot of displacement vs force as obtained from the laboratory testing.

At 424.1 seconds (the whole process lasts 440 seconds) the debonding is initiated. The reaction force starts to decrease reaching 0 in approximately 4 seconds. After this, theoretically, no further interaction between casing and cement should occur. However, this behavior is contradicted by the plot in Figure 8. After the debonding is initiated (when the force reaches 46,230 N) the applied force is still significant. This suggests that the debonding is not complete, there is still a certain bond between casing and cement.

This debonding can be explained in different ways. Since cement adhesions on the casing are detected for 10-25% of the initially bonded surface, it is a good guess that for the casing with adhesions to get out of the cement, a supplementary force is needed. Another possibility is that even after debonding, the interaction between the roughness of the casing and cement could produce that behavior.

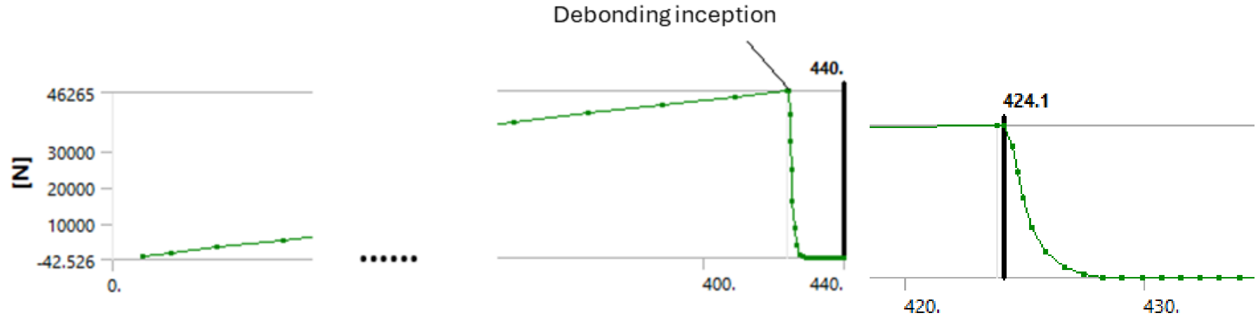

Figure 9: Reaction force at the cement base.

We tried to mimic such a behavior with a two-stage debonding. Since Ansys offers only a bilinear debonding curve, we tried another approach. We exported the stress distribution (via an External Data object) at the moment of the "first" deboning (at the moment when the displacement of the casing reached 7.5 mm to a new analysis, with a new CZM with the properties):

- Maximum Equivalent Tangential Contact Stress – 0.9 MPa;
- Tangential Slip at the Completion of Debonding – 2.5 mm

The force will start from 16,700 N. The reaction force at the cement base has the evolution presented in Figure 10. It can be seen that the results are in good accordance with the plot in Figure 8, where the force of 19,675 N is very close to the one resulting from the second debonding analysis (19,900 N). Better results can be obtained if further experiments are made and correlated with FEM analysis that will model the roughness of the casing-cement assembly.

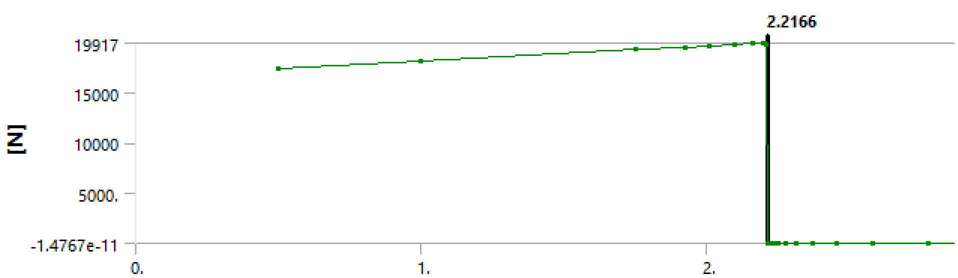

Figure 10: Reaction force at the cement base for the second debonding.

Teodoriu and Lambrescu (2023) have shown that once shear debonding is achieved (Type II contact) the casing acts independently from cement and thus the system loses its convergence or in other words, there is no more interaction between the casing and cement. However as observed in the laboratory work and field data, the casing still interacts with the cement after debonding. This interaction can be seen as a friction-induced effect. However, since there is no normal force between casing and cement after debonding, a friction model cannot explain the magnitude of the forces obtained, and thus as presented above we proposed the use of a two-stage CZM model.

Figure 11 presents the comparison of different methodologies regarding the wellhead growth phenomenon. The TOC was assumed to be at 1,600 ft while the 13-3/8" shoe was strictly at 1,629 ft. It can be seen that the calculation for the total length change of 13-3/8" does not considerably differ from the simulation results. Although the total length change of 7" during the hot production scenario due to temperature, ballooning, piston, and buckling effects was calculated to be 35", the simulation result yields 14.8" growth (i.e., where the growth of 7" production casing contributes just 14.8 in. – 13.3 in. = 1.5 inch to the wellhead movement). This shows that approximately 26% of the 7" production is expanding. The finite element simulation using simple CZM methodology presented by (Teodoriu & Lambrescu, 2023) have shown a total casing elongation of 31 inches, which is slightly lower than what we calculated by equation 2. This implies that a small elongation should exist with a two-stage CZM.

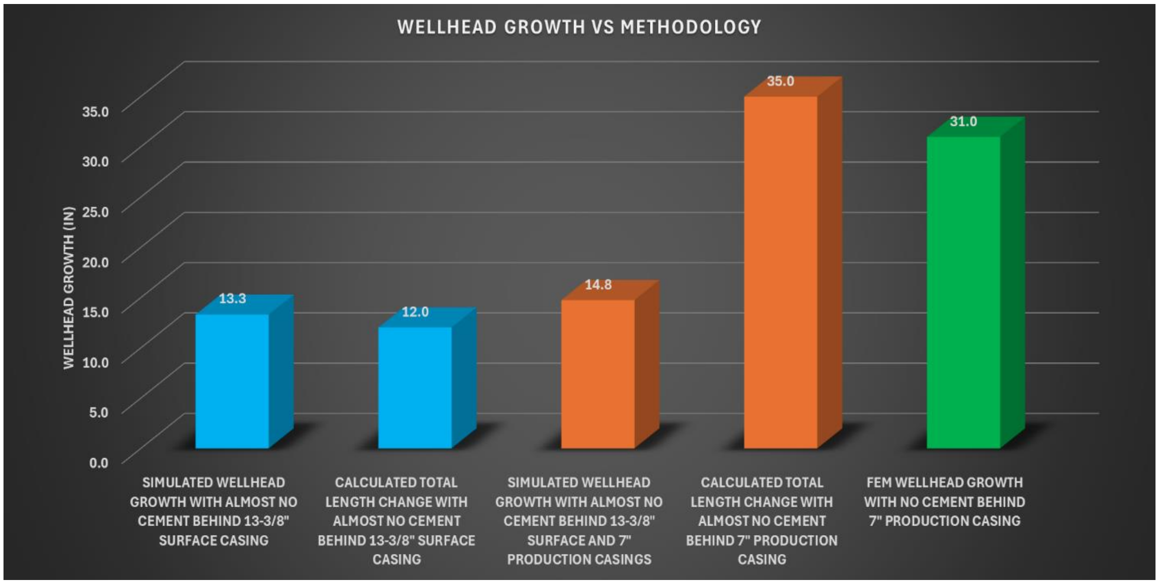

Figure 11: Analysis of wellhead growth under 10-year hot production. The amount of wellhead growth was determined based on the uncemented length factor "Q".

4. CONCLUSIONS

This paper shows that in the case of casing expansion, the total wellhead movement noticed at the surface cannot be estimated based on the linear expansion of production casing but rather requires a deeper understanding of the intimate interaction between casing and cement.

A finite element simulation was performed to understand the laboratory behavior of our tested samples, which shows a post-debonding high push force. The FEM uses for the first time a two-stage CZM model in which the casing-cement interaction is modeled also after debonding. The applied method shows clearly that after debonding the casing-cement will still interact, which as a result will lead to the conclusion that after debonding the casing thermal expansion will still be held by this post-debonding casing-cement interaction.

REFERENCES

Almulhem, K., Mrsic, Z., Thuwaibi, M., & Adesegha, R. (2020). Temperature Effect on HP Gas Well Integrity: Thermal Wellhead Growth Challenges and Solutions. SPE Asia Pacific Oil & Gas Conference and Exhibition,

ASME. (2010). Boiler and Pressure Vessel Code, Section VIII, Pressure Vessels (ASME: 2010). In.

Atlason, R. S., Geirsson, O. P., Elisson, A., & Unnthorsson, R. (2015). Geothermal Wellhead Maintenance: A Statistical Model Based on Documented Icelandic Experience. *Geothermics*, *53*, 147-153. https://doi.org/https://doi.org/10.1016/j.geothermics.2014.05.006

Cutrim, F. S., De Souza, C. O., & De Souza, B. S. P. (2021). Wellhead Movement Analysis and Surface Casing Integrity in Pre-Salt Wells. Offshore Technology Conference,

Gao, B.-k., Ren, J.-w., & Gao, L. (2016). Study on Wellhead Growth in Deep Well.

Godare, B. (1978). Geothermal Wellheads - the Heart of Geothermal Production Systems.

Halal, A. S., Mitchell, R. F., & Wagner, R. R. (1997). Multi-String Casing Design with Wellhead Movement. SPE Production Operations Symposium,

Hole, H. (2008). Geothermal Well Design - Casing and Wellhead. Petroleum Engineering Summer School Workshop,

Institute, A. P. (2011). Geotechnical and Foundation Design Considerations (API RP2 GEO: 2011). In: American Petroleum Institute.

Kaldal, G. S., Jonsson, M. T., Palsson, H., & Karlsdottir, S. N. (2015). Structural Modeling of the Casings in High-Temperature Geothermal Wells. *Geothermics*, *55*, 126-137. https://doi.org/https://doi.org/10.1016/j.geothermics.2015.02.003

Kaldal, G. S., Jónsson, M. Þ., Pálsson, H., & Karlsdóttir, S. N. (2015). Structural Analysis of Casings in High-Temperature Geothermal Wells in Iceland. Proceedings of World Geothermal Congress,

Kruszewski, M., Þórhallsson, S., Assadi, M., & Śliwa, T. (2017). Slimhole Well Casing Design for High-Temperature Geothermal Exploration and Reservoir Assessment. *AGH Drilling, Oil, Gas*, *34*(2), 465-493.

Liang, Q. J. (2012). Casing Thermal Stress and Wellhead Growth Behavior Analysis. SPE Asia Pacific Oil and Gas Conference and Exhibition,

McCabe, A. C. (1989). Well Vertical Movement on Platform Wells. SPE Offshore Europe,

McLennan, J. (2022). *Utah FORGE: Well 16A(78)-32 Stimulation Data (April 2022)* (Energy and Geoscience Institute at the University of Utah. https://doi.org/10.15121/1871203

McLennan, J., Nash, G., Moore, J., Skowron, G., & Woolsey, S. (2021). *Utah FORGE: Well 16A(78)-32 Drilling Data* (Energy and Geoscience Institute at the University of Utah. https://doi.org/10.15121/1776602

McSpadden, A. R., & Glover, S. (2009). Analysis of Complex Wellhead Load Events for Conductor and Surface Casing Strings. SPE/IADC Drilling Conference and Exhibition,

Proano, M. A., Meneses, A. R., Tates, V. A., Aponte, J., Magalhaes, T., & Duque, G. J. (2023). Prediction of Surface Wellhead Deformation via Calculation of Tubular Growth Due to Thermal Effects. SPE Western Regional Meeting,

Sathuvalli, U. B., & Suryanarayana, P. V. (2016). Structural-Casing/Soil Interaction Effects on Wellhead Motion. *SPE Drilling & Completion*, *31*(04), 273-285. https://doi.org/10.2118/180437-pa

Teodoriu, C., & Lambrescu, I. (2023). Numerical Investigations of Tensile Induced Debonding Due To Temperature Variation in Geothermal Wells. 48th Workshop on Geothermal Reservoir Engineering. Stanford University: Stanford University,

Þórhallsson, S. (2003). Geothermal Well Operation and Maintenance.

Unit, A. U. C. R. G. C. (2016). The African Union Code of Practice for Geothermal Drilling. In.

Watson, A. (2013). Geothermal Drilling and Well Design. In A. Watson (Ed.), *Geothermal Engineering: Fundamentals and Applications* (pp. 77-97). Springer New York. https://doi.org/10.1007/978-1-4614-8569-8_5

Williams, J. (1991). Geothermal Wellheads: Tough Equipment for a Rough Environment. *Geothermal Resources Council Bulletin*, *May*, 143-146.

Winkler, D., Swearingen, L., & McLennan, J. (2021). *Utah FORGE: Well 16A(78)-32: Summary of Drilling Activities* (Energy and Geoscience Institute at the University of Utah. https://gdr.openei.org/submissions/

Zhang, Z., Zhou, Z., He, Y., & Zhou, J. (2017). Study of a Model of Wellhead Growth in Offshore Oil and Gas Wells. *Journal of Petroleum Science and Engineering*, *158*, 144-151. https://doi.org/https://doi.org/10.1016/j.petrol.2017.08.042

Zhou, N., Deng, K., Lin, Y., Yan, K., Li, C., Li, H., & Xie, P. (2024). A Prediction Method of Wellhead Movement with Consideration of Interface Debonding. *Geoenergy Science and Engineering*, *239*, 212919. https://doi.org/https://doi.org/10.1016/j.geoen.2024.212919